Mechanical Anisotropies of Laminated Sedimentary Rocks

M. E. CHENEVERT*
JUNIOR MEMBER AIME
C. GATLIN**
MEMBER AIME

THE U. OF TEXAS
AUSTIN, TEX.

ABSTRACT

The effects of bedding plane orientation on the elastic constants and the yield strengths of three laminated rocks (one sandstone and two shales) and one isotropic rock (a limestone) were studied. The directional dependence of the elastic properties of these rocks was experimentally evaluated using a triaxial compression cell and auxiliary stress-strain measuring equipment. Symmetry of Poisson's ratios within the bedding plane suggested that horizontal isotropy exists, but the bedding planes do give rise to an appreciable difference between properties in the horizontal and vertical directions. For the three bedded rocks studied, Young's modulus was lower normal to bedding than along bedding.

Yield strengths were determined at confining pressures from 0 to 12,000 psi in a triaxial compression cell. The rocks studied showed strength reductions as high as 40 per cent when the test specimen was oriented at 20°–30° to the bedding planes. The mechanical behavior of these rocks suggested that the rock properties of shear strength and/or coefficient of internal friction can vary with direction, depending on the particular rock tested. Tensile strengths were also measured and found to be lowest when failure occurred along bedding.

This work shows that bedded formations exhibit sizable directional variations in both their elastic constants and yield strengths. It is suggested that these variations may be accounted for by using the "elastic laminate" model and the "variable coefficients" failure model.

INTRODUCTION

The nature of rock deformation at elevated pressures has been studied by many workers; papers by Handin,[1,2] and Robinson[3] illustrate the present state of knowledge. Most investigators have either chosen rocks which were as isotropic as possible (in order to avoid complications of data interpretation and analysis) or they have oriented their samples so that the effects of anisotropies (such as bedding planes) have been avoided. Of the studies performed, few were concerned specifically with mechanical anisotropies.

Griggs[4] has presented limited data for specimens cut parallel, normal, and 45° to the bedding plane; he relates the strength anisotropy observed to the fabric (bedding) anisotropy. His tests were primarily concerned with large deformations (20 per cent strain); thus, no directional values of the elastic constants were reported. Handin has reported the results of similar experiments. Bott[5] has discussed rock strength anisotropies due to faults, cleavage, or bedding. He was concerned primarily with determining the shear stress on such planes and did not mention the effect of friction. Jaeger[6] later generalized Bott's work by taking friction into account and presented a limited theory for the failure of rocks having a "single plane of weakness", and also for rocks having a constant coefficient of friction, and a shear strength which varies with bedding plane orientation.

Donath and Cohen,[7] and Donath[8] have evaluated rock strengths from shale and slate specimens cut normal and parallel to bedding. A dependence of cohesive strength (τ_o) on the specimen orientation was also shown. Adler[9] has also studied this problem and lists similar results. He assumes that all bedded rocks behave according to Jaeger's single-plane-of-weakness theory. Kalinin and Belorussov[10] list results for strength tests parallel and perpendicular to bedding and use this information as a basis for hole deviation analysis.

From the literature it is apparent that sedimentary rocks have been tested under widely varying conditions of stress; however, the assumption of isotropy is generally, but not always, made. Since geologic sedimentation often deposits sediments in very definite layers, it seems that more systematic attention should be given to the possible effects of this natural bedding. Bedding, as used here, refers to visible regularities of grain size or orientation resulting from depositional processes. The mechanical strength anisotropies, which bedding may present, is not the only anisotropic property to be considered, since the elastic

Original manuscript received in Society of Petroleum Engineers office Aug. 3, 1964. Revised manuscript received Feb. 8, 1965. Paper presented at 39th Annual Fall Meeting of SPE in Houston, Tex., Oct. 11-14, 1964.

*Currently with Esso Production Research Co., Houston, Tex.
**Currently with Drexel Institute of Technology, Philadelphia, Pa.

[1]References given at end of paper. SPE 890

"constants" may also have directional dependence.

The primary objective of this study was to investigate the directional dependence of the physical properties of several laminated rocks in the hope of determining whether or not these effects are of sufficient magnitude to be considered in engineering applications.

ELASTIC CONSTANT DETERMINATIONS

In the linear theory of elasticity for isotropic, homogeneous solids only two elastic constants of the material are needed. These are, of course, E (Young's modulus) and ν (Poisson's ratio). This two-constant simplification of the general rheological model for a completely anisotropic (36 "constants") solid is obtained by applying various simplifying assumptions to the generalized Hooke's law.[11] Between these degrees of complexity are possible many other rheological or continuum mechanics models, one of which is the orthotropic body. This particular model exhibits three mutually perpendicular planes of elastic symmetry, which can be shown to require nine independent elastic constants for complete specification. Wood, as an example, is often described as being orthotropic; various engineering laminates (plywood) are also reasonably orthotropic.[12] The standard mathematical formulation for an orthotropic body shows that the stress-strain relations are given by the equations[13]

$$\epsilon_x = \frac{\sigma_x}{E_x} - \frac{\sigma_y \nu_{yx}}{E_y} - \frac{\sigma_z \nu_{zx}}{E_z} , \quad . . . \quad (1)$$

$$\epsilon_y = \frac{\sigma_y}{E_y} - \frac{\sigma_x \nu_{xy}}{E_x} - \frac{\sigma_z \nu_{zy}}{E_z} , \quad . . . \quad (2)$$

$$\epsilon_z = \frac{\sigma_z}{E_z} - \frac{\sigma_x \nu_{xz}}{E_x} - \frac{\sigma_y \nu_{yz}}{E_y} , \quad . . . \quad (3)$$

$$\tau_{xy} = C_{xy} \alpha_{xy} , \quad . . . . . \quad (4)$$

$$\tau_{yz} = C_{yz} \alpha_{yz} , \quad . . . . . \quad (5)$$

$$\tau_{zx} = C_{zx} \alpha_{zx} , \quad . . . . . \quad (6)$$

where $\epsilon_{x,y,z}$ are the longitudinal strains associated with the three principal stresses $\sigma_{x,y,z}$, the magnitude of which is governed by Young's moduli $E_{x,y,z}$, and Poisson's ratios $\nu_{yx,yz,xy,xz,zx,zy}$. The constant E_i denotes a value of Young's modulus computed from $E_i = \sigma_i/\epsilon_i$. Poisson's ratio requires a double subscript notation; the first subscript denotes the direction in which the actuating stress acts, and the second subscript denotes the direction in which the lateral strain is measured. Shearing stresses $\tau_{xy,yz,zx}$ are related to the shearing strains $\alpha_{xy,yz,zx}$ through the constants $C_{xy,yz,zx}$, as given in Eqs. 4 through 6. These shear constants could not be evaluated with the triaxial compression cell used in this work.

By use of the strain-energy density function it is possible to show that the normal elastic constants are related by the following equations.[13]

$$\frac{\nu_{yx}}{E_y} = \frac{\nu_{xy}}{E_x} , \quad . . . . . \quad (7)$$

$$\frac{\nu_{xz}}{E_x} = \frac{\nu_{zx}}{E_z} , \quad . . . . . \quad (8)$$

$$\frac{\nu_{yz}}{E_y} = \frac{\nu_{zy}}{E_z} , \quad . . . . . \quad (9)$$

Thus, it is possible to reduce the nine constants given in Eqs. 1 through 3 to six independent elastic constants. These six constants plus the three shear constants comprise the nine independent elastic constants needed to completely describe the elastic behavior of an orthotropic solid.

Laminar similarities between wood and rocks such as shale suggest that the orthotropic model might be more applicable to some rocks than the usually applied isotropic model. While this particular study was primarily concerned with strength anomalies, the elastic behavior of four rocks was also studied. Direct measurements of axial stress and the resulting axial and lateral strains permitted determination of the elastic constants associated with normal stresses.

EXPERIMENTAL PROCEDURE

An adaptation of Robinson's triaxial cell[3] was used in all high-pressure measurements described in this paper. Lateral strains were measured with a radial displacement indicator designed by E. A. Ripperger and his students at The U. of Texas. This device is similar to a C-clamp with four strain gauges mounted on its throat and is actuated by the lateral strain of the test specimen. Lateral strains (and, hence, Poisson's ratios) were measured only at atmospheric conditions. Careful calibration of the triaxial cell permitted determination of longitudinal strain (and, hence, Young's moduli) at elevated confining pressures. Details of these procedures are available elsewhere.[13]

ROCK DESCRIPTIONS

Leuders Limestone

Leuders limestone (from quarries near Leuders, Tex.) shows no apparent orientation in structure and was studied primarily to give a comparison between an isotropic rock and those considered as orthotropic. Its availability and previous use

by our laboratories[15-17] were also factors in its selection. Of Permian age, it is a light gray, fossiliferous limestone. Its fossil content is 80 to 90 per cent. The porosity is approximately 20 per cent and the permeability less than 1 md.

Green River Shale

Green River shale was procured from the Bureau of Mines demonstration mine near Rifle, Colo. It was deposited in two large, shallow, fresh-water lakes, and is a light gray and light brown, thinly banded, finely laminated oil shale (Fig. 1). It is chiefly composed of very fine-grained calcite and dolomite.

Arkansas Sandstone

The Arkansas sandstone used was quarried in Logan County, Ark. This Pennsylvanian Age rock is a fine-grained, highly cemented sandstone consisting of 95.2 per cent silica, 1.33 per cent moisture, 0.6 per cent iron oxide and 2.5 per cent alumina. It is reddish-brown, lightly banded, and has a permeability of less than 0.5 md. It breaks easily along iron oxide deposits which occur along bedding every 2 to 6 in. apart. Within the 2-in. thick slab used in this study, there appeared to be no fractures or iron oxide layers.

Permian Shale

The Permian shale sample was obtained from Shell Oil Co. and was cored in Ector County, Tex., at a depth of 7,302 ft. It is dark gray, thinly banded, finely laminated, and has a permeability of less than 0.5 md. The bulk core was 3½-in. in diameter and 8-in. long, so the number of test specimens were few.

SAMPLE PREPARATION

From each sedimentary rock studied, specimens were drilled with a ¾-in. diamond core barrel using kerosene as the cooling fluid (to eliminate clay hydration). For each formation studied, all test specimens were cut from the same slab in order to minimize compositional variations. As shown in Fig. 1, specimens cut parallel to bedding were designated by either *X* or *Z*. It was assumed that these orientations were the orthotropic axes of the rock. The visual bedding planes gave a definite indication of the *Y* direction (normal to bedding), but the *X* and *Z* directions were chosen arbitrarily. This proved to be permissible because the rocks tested showed no significant variation of physical properties in the *X-Z* plane. Specimens were also cut at angles of 15°, 30°, 45°, 60° and 75° to the bedding plane. These were all cut in the *X-Y* plane, and were designated by a notation such as "S-30°-3"; this notation means Specimen No. 3 was cut from a slab of Arkansas sandstone (S) at an angle of 30° to the bedding plane.

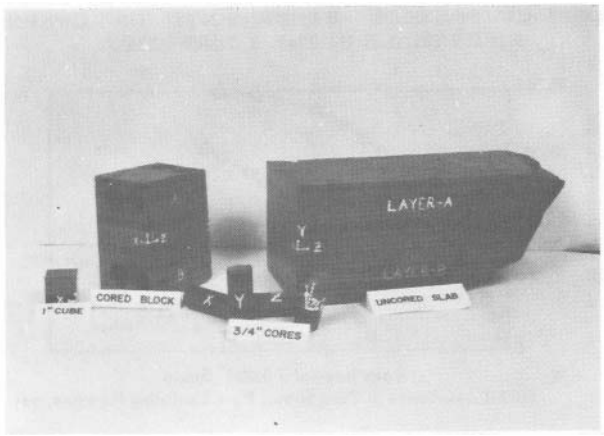

FIG. 1 — PREPARATION OF GREEN RIVER SHALE SAMPLES FROM QUARRY BLOCK.

After the cores were removed from the slab they were trimmed to an approximate length of 1½ in. with a diamond saw, again using kerosene as a cooling fluid.

The standard specimen length-to-diameter ratio of 2.0 was used to eliminate any effect of specimen length on compressive strength. Ends of the cores were ground flat and parallel to a tolerance of 0.001 in. — a very necessary step to ensure proper loading. Cubes of rock (Fig. 1) were also used to determine elastic constants. Pore pressure was zero and the rocks were unsaturated in all tests reported herein.

Special tests were performed on 1½ in. cubes of Arkansas sandstone in order to check earlier elastic constant results which did not agree with the strain-energy density function concept. We found it necessary to lap these cubes to within 0.0002-in. tolerance in order to achieve consistent results.

EXPERIMENTAL RESULTS — ELASTIC CONSTANTS

In analyzing the data we assumed that the specimen initially behaved in a linearly elastic manner. This assumption was reasonably substantiated by the linear stress vs strain (radial and axial) curves determined, as typically shown in the initial portion of the stress-strain curves of Figs. 3 through 6. All rocks tested exhibited this linear relationship during the early portion of the stress-strain curve; this was followed by a nonlinear portion. The phenomenon of stress-strain hysterisis

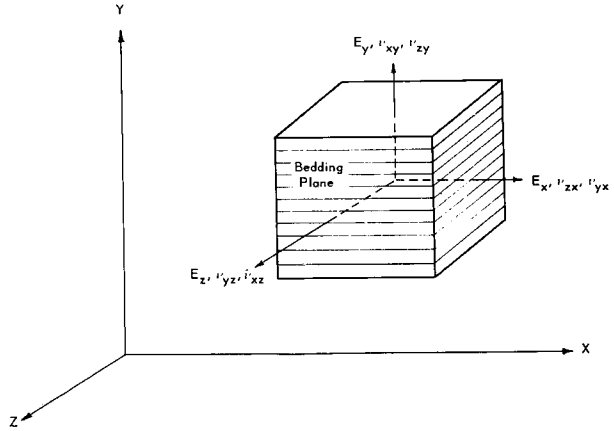

FIG. 2 — DIRECTIONS OF ELASTIC CONSTANTS.

was not investigated.

Average results of all elastic constant determinations are given in Table 1. These include values of E at all confining pressures, since pressure proved to have an unmeasurable effect on Young's modulus for any of the test rocks. The Appendix (Table A-1) gives a more complete listing of these data.

Leuders limestone was found to be essentially isotropic and fairly homogeneous; hence, the single values of E and ν were adequate.

The other three rocks studied, all bedded rocks, behaved in a similar manner. Values of Young's moduli normal (E_y) and parallel (E_x, E_z) to the bedding were appreciably different, with E_y always being lower. Symmetry of Poisson's ratios existed in the X-Z plane, suggesting that horizontal isotropy exists, but the bedding planes did give rise to an appreciable difference between properties in the horizontal and vertical directions. This particular behavior is what one might expect from an orthotropic model which has a single plane of isotropy and might be referred to as a "laminated model". The five elastic constants used to describe each laminate rock in Table 1 can be further reduced to four through the use of the strain-energy density function.

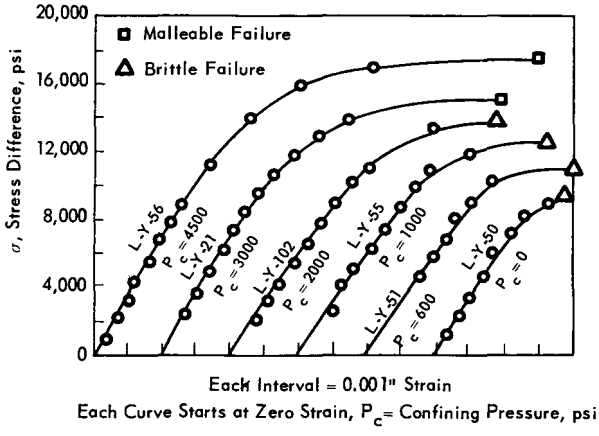

FIG. 3 — TYPICAL STRESS-STRAIN CURVES FROM AXIAL COMPRESSION EXPERIMENTS OF LEUDERS LIMESTONE SPECIMENS, Y DIRECTION.

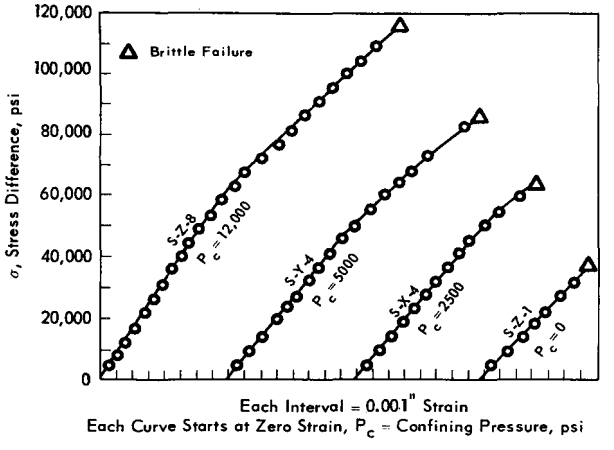

FIG. 4 — TYPICAL STRESS-STRAIN CURVES FROM AXIAL COMPRESSION EXPERIMENTS ON ARKANSAS SANDSTONE SPECIMENS.

TABLE 1 — SUMMARY OF ELASTIC PARAMETERS

Rock	Elastic Parameters	
	E, 10^6 psi	ν
Leuders limestone (Isotropic)	3.6	0.20
Arkansas sandstone (Laminate)	$E_y = 2.8$ $E_x \cong E_z = 4.6$	$\nu_{yx} \cong \nu_{yz} = 0.13$ $\nu_{xy} \cong \nu_{zy} = 0.20$ $\nu_{xz} \cong \nu_{zx} = 0.15$
Green River shale (Laminate)	$E_y = 4.3$ $E_x \cong E_z = 5.1$	$\nu_{yx} \cong \nu_{yz} = 0.18$ $\nu_{xy} \cong \nu_{zy} = 0.19$ $\nu_{xz} \cong \nu_{zx} = 0.15$
Permian shale (Laminate)	$E_y = 3.5$ $E_x \cong E_z = 4.8$	$\nu_{yx} \cong \nu_{yz} = 0.13$ $\nu_{xy} \cong \nu_{zy} = 0.21$ $\nu_{xz} \cong \nu_{zx} = 0.18$

The results of Table 1 show the hazards of generalizing on the rheology of rocks, and clearly suggest that the usually applied isotropic model may not be adequate to describe the behavior of shales. However, the orthotropic model (nine constants) may be simplified to a laminate model (four constants) through the use of the strain-energy density function and the assumption of horizontal isotropy.

YIELD STRENGTH AND FAILURE MECHANICS

Extensive series of tests were run on each of

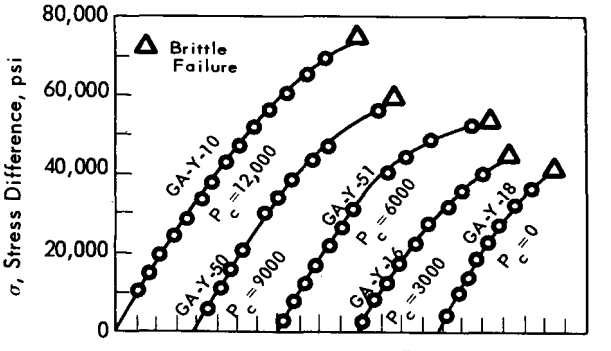

FIG. 5 — TYPICAL STRESS-STRAIN CURVES FROM AXIAL-COMPRESSION EXPERIMENTS OF GREEN RIVER SHALE IN THE Y DIRECTION.

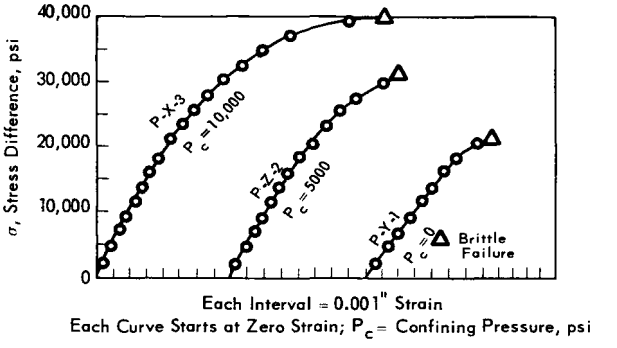

FIG. 6 — TYPICAL STRESS-STRAIN CURVES FROM AXIAL COMPRESSION EXPERIMENTS OF PERMIAN SHALE.

the above rocks to determine both yield strength and failure mode. In the case of elastic stress-strain behavior followed by brittle fracture, yield strength and fracture strength were identical. In cases where appreciable plastic strain occurred, the yield strength was taken as the stress at 0.20 per cent strain offset, as is customary in the metals industry.[18]

The only failure theories found to be useful in analyzing experimental data were those of Griffith,[14] Jaeger,[6] and the well-known Mohr-Coulomb theory from soil mechanics. Applications of these theories will be presented in conjunction with the discussion of the experimental results.

EXPERIMENTAL RESULTS

Typical stress-strain curves for the various rocks are given in Figs. 3 through 6. The stress difference plotted on the ordinate is the axial stress less the confining pressure. Only the Leuders limestone exhibited any large degree of plasticity. Since it is difficult to generalize, the experimental results will be discussed in turn for each rock.

Leuders Limestone

As shown in Fig. 3, this limestone has a uniaxial compressive strength of about 10,000 psi, and tends to become plastic at confining pressures greater than 3,000 psi, Fig. 7 shows typical specimen failures, which were quite brittle under atmospheric conditions, yet flowed plastically at high confining pressures. Typical "cones of fracture" were experienced, as reported by Robinson. Samples L-Z-1, L-X-9 and L-Z-4 are good examples of brittle failure. Sample L-Y-20 is a good example of plastic flow as shown by the large strain without fracture, and plastic flow lines which appear on its surface. Sample L-Z-41 should probably be considered in the "transition zone" between brittle and plastic failure; shear planes are present, yet the rock still possesses cohesive strength. Sample L-Z-1 is a good example of a brittle failure under atmospheric conditions. a single shear plane is first developed, and is followed by extensive splintering.

Arkansas Sandstone

This sandstone had a uniaxial compressive strength of 35,000 psi and exhibited brittle failure for all values of confining pressure, as shown in Fig. 4. A confining pressure of 12,000 psi raised the compressive yield strength to about 130,000 psi, a fourfold increase. The high strength of this rock is explained by its composition being 95 per cent quartz. Tests were conducted at confining pressures up to 12,000 psi, and for 15° bedding plane orientations up to $\beta = 90°$, where β is the angle which the bedding plane makes with the cylindrical axis of the specimen. Failure occured along the bedding planes for $\beta = 15°$ and 30° only. Specimens S-75°-4, S-90°-3 and S-Y-8 of Fig. 8 exhibit typical conjugate failure planes as evidenced by the "V" formed by the two shear planes. This was usually observed for shear failure across bedding planes. Specimen S-30°-3 does not have conjugate failure planes, and represents typical failure along a bedding plane.

Specimen S-Z-2 is typical of failure in a laminated rock where $\beta = 0°$. A single shear plane exists across the rock and is intersected by many failure planes which occur along the bedding of the rock. most tests of this type resulted in a completely splintered specimen from which it was impossible to measure the initial failure plane. This splintering is believed to be caused by the high coefficient of friction which exists along the failure plane for this orientation. Specimen S-75°-4 broke into three pieces; thus, it was possible to reconstruct the rock as shown. Specimen S-Y-8, which was deformed at a confining pressure of 12,000 psi, was classified as failure in the transition zone between brittle and plastic failure.

Green River Shale

Fig. 5 shows typical stress-strain curves for Green River shale. The curves become nonlinear at a stress difference of about 20,000 psi and continued as such until failure. These shale specimens were still elastic in the nonlinear region, as determined by cyclical tests in which the samples were repeatedly loaded and unloaded with the same nonlinear stress-strain curves being obtained in each case with no permanent set observed. This oil shale exhibited brittle failure at all values of confining pressure (the failures were quite similar to those of the Arkansas sandstone). Smooth failure planes were observed for tests performed at high confining pressures (greater than 10,000 psi), regardless of the orientation.

Permian Shale

As shown in Fig. 6, the Permian shale had a uniaxial compressive strength of about 20,000 psi, and it exhibited brittle failure for all values of confining pressure. Only one test could be run at each point because of the small quantity of material available. A "soft" rock, this shale gave "clean" failures with little of the splintering characteristics of "hard" rocks.

DISCUSSION OF EXPERIMENTAL RESULTS

The various theories summarized by Robertson[19] were applied to all rocks tested. It was found that either the Griffith theory or the Mohr-Coulomb approach could be applied to the Leuders limestone. On the other hand, the Arkansas sandstone was better represented by the Jaeger's single-plane-of-weakness theory. The Green River shale had an internal coefficient of friction which varied with direction. It was impossible to obtain sufficient data on the Permian shale to determine whether its coefficient of internal friction and cohesive strength were continuously variable. Thus, both the single-

plane-of-weakness and the variable-coefficient approaches were applied, and the results compared. The failure theory of Griffith was applied to the Arkansas sandstone, the Green River shale and the Permian shale with little success.

When a specimen fails along a bedding plane, it is necessary to take a few precautions in developing the envelops to the Mohr failure circles. It is quite possible that the curve which connects the failure conditions of each Mohr circle is not tangent to the Mohr circles. Fig. 9 is a good example of this concept. As is shown, the Mohr circles are drawn in the usual manner along the σ_n axis. The specimens failed along the bedding planes, which were oriented at an angle of $\beta = 30°$. Thus, the normal stress σ_n acting across this plane and the shearing stress τ acting along this plane are determined by the graphical method of Mohr. A radius is drawn through each circle at an angle of 2θ (60°) to the σ_n axis. The point at which each radius intersects the Mohr circle gives the stresses acting on the failure plane. The line which connects the failure conditions of each circle represents the locus of the points which satisfy the modified Mohr-Coulomb equation

$$\tau = \tau_o' - \sigma_n \tan \phi' \quad \cdots (10)$$

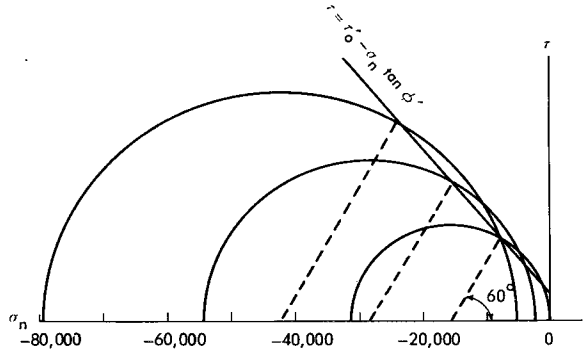

FIG. 9 — CONSTRUCTION OF MOHR'S ENVELOPE FOR ARKANSAS SANDSTONE WITH $\beta = 30°$. FAILURE OCCURS ALONG BEDDING PLANE.

where τ_o' represents the cohesive strength of the material along the bedding plane, σ_n is the effective normal stress (compression being negative), and tan ϕ' represents the coefficient of internal friction along the bedding plane. In the Jaeger single-plane-of-weakness theory[6] this equation is used for all failures which occur along bedding, and the usual Mohr-Coulomb equation

$$\tau = \tau_o - \sigma_n \tan \phi \quad \cdots (11)$$

is used for all failures which occur across bedding, where τ_o and tan ϕ represent the cohesive strength

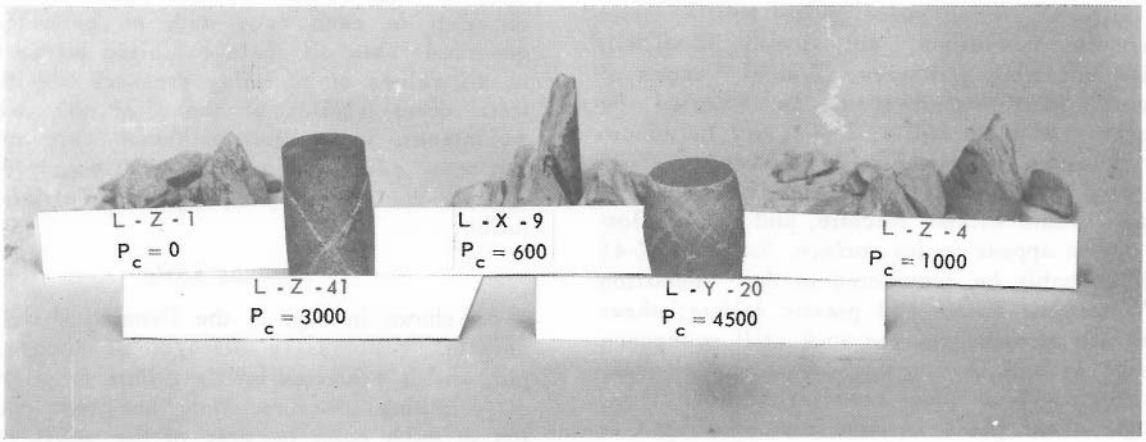

FIG. 7 — LEUDERS LIMESTONE SPECIMENS AFTER COMPRESSION AT VARIOUS CONFINING PRESSURES.

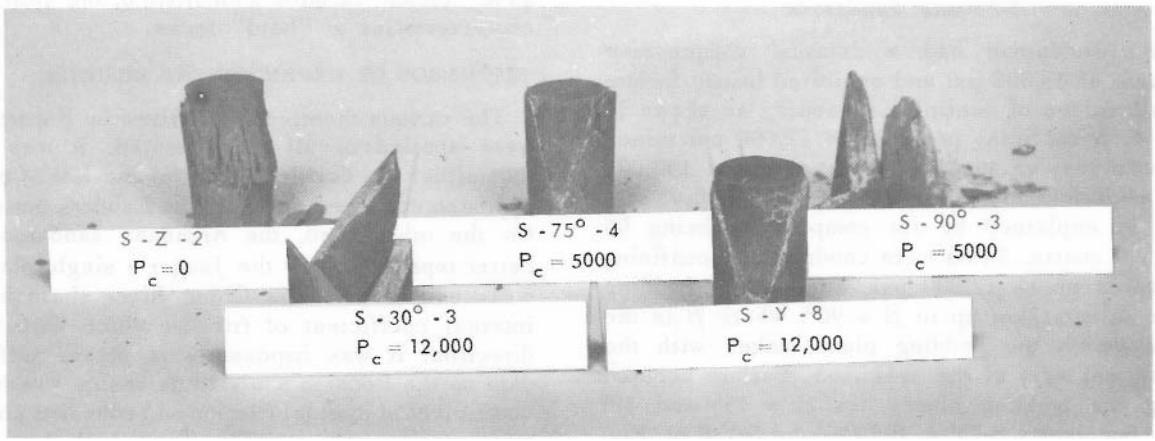

FIG. 8 — ARKANSAS SANDSTONE SPECIMENS AFTER COMPRESSION AT VARIOUS CONFINING PRESSURES.

and coefficient of internal friction, respectively, across the bedding planes. A detailed analysis of test data for each rock follows.

Leuders Limestone

The Griffith failure criterion states that if

$$(3\sigma_1 + \sigma_3) > 0 \quad \ldots\ldots\ldots (12)$$

rupture occurs when $\sigma_1 = K$.

If $(3\sigma_1 + \sigma_3) < 0$, rupture occurs when

$$(\sigma_1 - \sigma_3)^2 + 8K(\sigma_1 + \sigma_3) = 0 \quad \ldots (13)$$

where σ_3 = axial stress,

σ_1 = confining pressure, and

K = uniaxial tensile strength of the rock.

In triaxial compression tests both σ_1 and σ_3 are negative; therefore, only the second of the above failure criteria can be applied. Fig. 10 shows Eq. 13 compared with experimental data, and as shown, Griffith's theory describes failure in Leuders limestone fairly well. The Mohr envelope also describes the behavior of the Leuders with reasonable accuracy (Fig. 11).

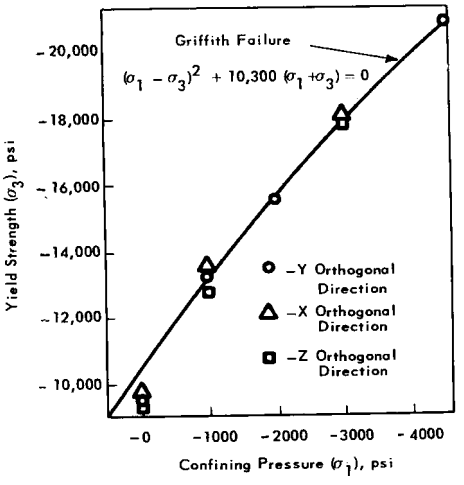

FIG. 10 — COMPARISON OF EXPERIMENTAL RESULTS FOR LEUDERS LIMESTONE TO FAILURE THEORY OF GRIFFITH.

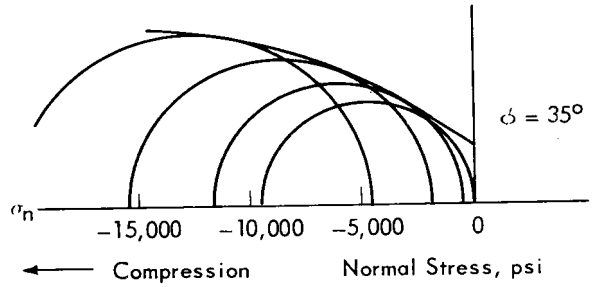

FIG. 11 — MOHR'S ENVELOPE FOR LEUDERS LIMESTONE.

Arkansas Sandstone

The anisotropic-shear-failure theory of Jaeger applied only to the Arkansas sandstone. It was possible to orient (prepare) the specimen so that the failure plane was the bedding plane, thereby facilitating the measurement of strength and related properties along the bedding plane. It was not possible to run these tests at confining pressures in excess of 5,000 psi, because of equipment limitations. In trial tests several points at 12,000 psi were obtained, but in each case the sandstone "wedge", which was formed at failure, damaged the piston face. This was particularly true for those specimens cut at $\beta = 30°$.

Coulomb envelopes were developed for seven values of β at 15° intervals, and the results were plotted to form the composite diagram of Fig. 12. As previously explained, care must be taken in the construction of the failure envelopes. The particular arrangement of the envelopes of Fig. 12 suggested that this material behaved as though it were isotropic except for a single plane of weakness. Fig. 13 gives a graphic interpretation of the single-plane-of-weakness theory. The heavy lines are those predicted by theory (Eqs. 10 and 11) where the constants τ_o and ϕ were determined from the $\beta = 90°$ curve of Fig. 12. The $\beta = 30°$ curve of Fig. 12 was used to evaluate τ_o' and ϕ'. The points shown in Fig. 13 are experimental data. The theoretically predicted minimum yield strength occurs for $\beta = 20°$, but unfortunately no experiments were performed at this orientation. The data points for $\beta = 0°$ are consistently high, which is probably caused by an increase in the coefficient of friction for this particular type of failure. This frictional effect is explained in detail later.

Although the Arkansas sandstone had no "fractures" (planes of weakness), as determined by visual observations and tensile strength tests, it was described reasonably well by the Jaeger theory.

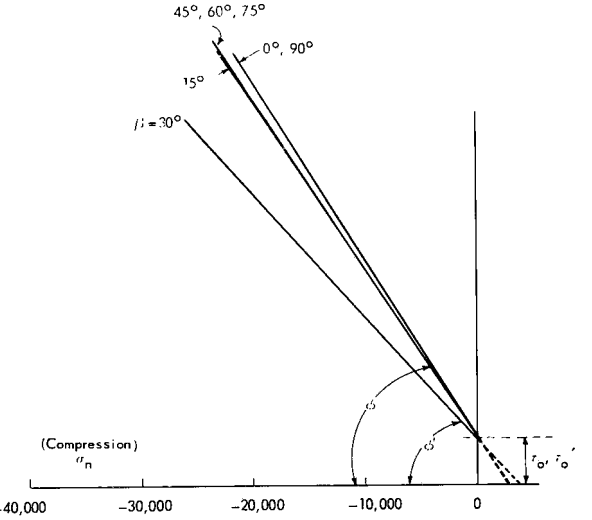

FIG. 12 — COULOMB'S ENVELOPES FOR ARKANSAS SANDSTONE WITH $\beta = 0°$, 15°, 30°, 45°, 60°, 75° AND 90°.

Green River Shale

Compression tests were run on this rock at confining pressure up to 12,000 psi and for 15° values of β. As shown in Fig. 14, this rock experienced a minimum yield strength at $\beta = 30°$ (approximately 30 per cent less than the yield strength at $\beta = 90°$).

The linear portion of all failure envelopes for this oil shale is plotted on a single axis in Fig. 15. This figure suggested that the Green River shale did not behave as a rock with a single plane of weakness but, rather, as one with a continually varying coefficient of friction, tan ϕ. Another interesting point of Fig. 15 is that the cohesive strength τ_o, varies only slightly with orientation β, and may be considered as a constant equal to 7,500 psi. Fig. 14 also suggested this, since the curves shown there do not have the shape predicted by the single-plane-of-weakness theory (see Fig. 13). It is believed that the yield strength data trends of Fig. 14 are what one would usually expect for a shale. Donath[8] has reported similar results for a slate and a shale.

Fig. 16 shows graphically the variation of tan ϕ with the angle γ which is the angle between the bedding and failure planes:

$$\gamma = \beta - \theta = \beta - \frac{\frac{\pi}{2} - \phi}{2} \quad \ldots . (14)$$

As is seen in Fig. 16, tan ϕ varies from a value of 0.58 to 0.93 over the range $-25° < \gamma < 68°$, with the minimum occurring at $\gamma = 0°$. This is the entire range which can be investigated for the Green River shale with triaxial testing equipment.

Notice that the data of Fig. 16 are not symmetric about the $\gamma = 0°$ axis. At first thought it would

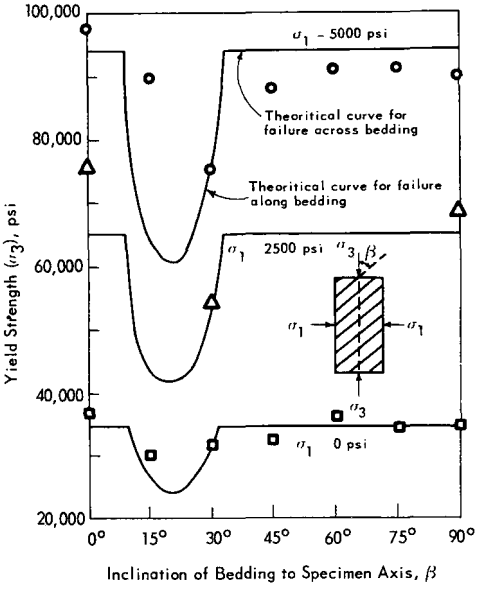

FIG. 13 — COMPARISON OF ARKANSAS SANDSTONE EXPERIMENTAL DATA TO SINGLE-PLANE-OF-WEAKNESS THEORY AT VARIOUS CONFINING PRESSURES (σ_1) AND INCLINATIONS OF BEDDING PLANES (β).

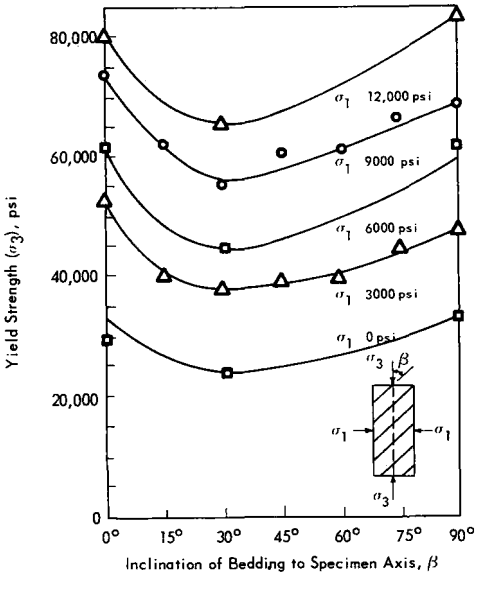

FIG. 14 — YIELD STRENGTH VS INCLINATION OF BEDDING PLANES, β, FOR GREEN RIVER SHALE AT VARIOUS CONFINING PRESSURES.

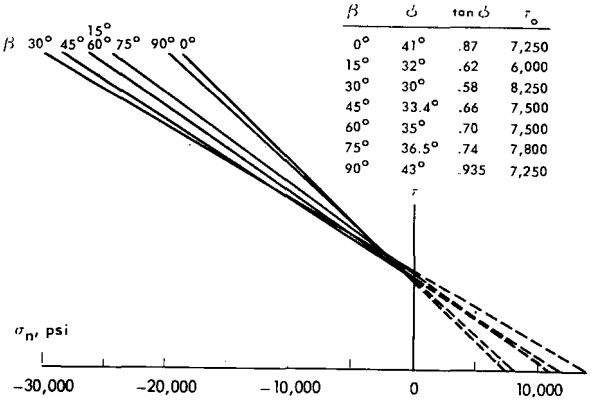

β	ϕ	tan ϕ	τ_o
0°	41°	.87	7,250
15°	32°	.62	6,000
30°	30°	.58	8,250
45°	33.4°	.66	7,500
60°	35°	.70	7,500
75°	36.5°	.74	7,800
90°	43°	.935	7,250

FIG. 15 — MOHR'S ENVELOPES FOR GREEN RIVER SHALE FOR $\beta = 0°$, 15°, 30°, 45°, 75° AND 90°.

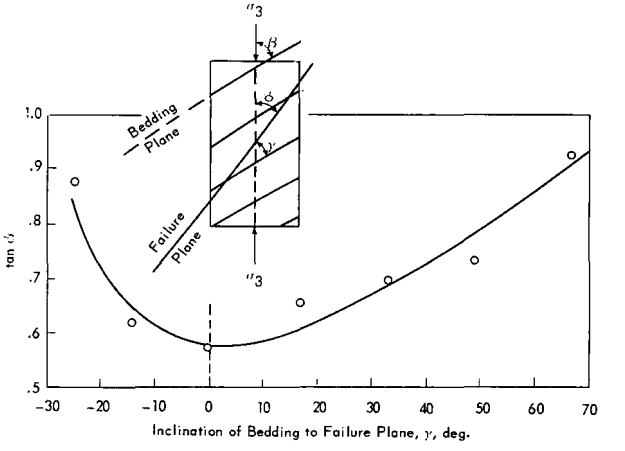

FIG. 16 — VARIATION OF COEFFICIENT OF FRICTION WITH INCLINATION OF BEDDING TO FAILURE PLANE γ FOR GREEN RIVER SHALE.

appear logical that the same value of tan ϕ should be measured for negative or positive values of γ. This departure from symmetry may be explained qualitatively as follows. Consider diagrams A, B, C and D of Fig. 17. Diagram A shows the case where failure has occurred along the bedding plane, resulting in a minimum value of tan ϕ. Diagram B shows the case for failure perpendicular to bedding, and a high value of tan ϕ is recorded. Diagrams C and D show failure for situations intermediate between A and B. The value of tan ϕ for Case D is higher than that of Case C because of the direction of relative motion between the two surfaces in contact. In Case C the individual layers are pointed away from the direction of movement. In Case D the individual layers are pointed together, thereby causing penetration or interlocking of lamina, and ultimate splintering. A similar directional coefficient of friction has been observed by workers in the fiber industry.[20] From this analysis it would be expected that the yield strength at $\beta = 0°$ is greater than for $\beta = 90°$, which was observed (Fig. 13 and 14).

The observations for the Green River shale (variable tan ϕ and constant τ_o) are not always observed in other laminated rocks. Donath[8] reports both a variable tan ϕ and a variable τ_o for the Martinsburg slate. In a generalization of the single-plane-of-weakness theory, Jaeger assumes tan ϕ is constant and τ_o varies with bedding plane orientation. Values of tan ϕ varied from 0.58 to 0.93 for the Green River shale, and τ_o varied from 2,700 to 5,500 psi for the Permian shale. Therefore, as an approximation, one may expect these rock properties (τ_o and tan ϕ) to vary by as much as 50 per cent.

Permian Shale

Compression tests were conducted on Permian shale at confining pressures of 0, 5,000 and 10,000 psi, and for values of $\beta = 0°$, 30° and 90°. As previously mentioned, all specimens were cut from a 4½-in oilwell core, so only a few test specimens could be obtained. The linear portion of typical Mohr envelopes is shown in the composite diagram of Fig. 18. From the data obtained, it was not possible to determine if this rock could best be treated as one with a single plane of weakness, or as one with a variable coefficient of friction and/or cohesive strength. Analysis showed that for this shale, τ_o varied with β (Fig. 19), but for practical purposes tan ϕ did not.

A comparison of these two methods is shown in Fig. 20, where Curves A and B apply to the single-plane-of-weakness theory and Curve C applies to the variable-coefficients approach. Disagreement between the two predictions exists in the regions $45° < \beta < 75°$ and $5° < \beta < 15°$. This approach of using both methods in conjunction

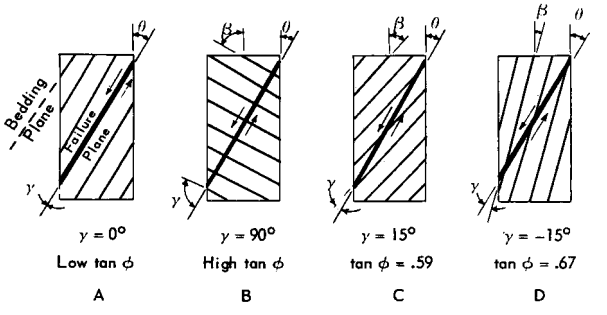

FIG. 17 — COEFFICIENT OF FRICTION VARIATIONS AS ILLUSTRATED BY VARIATIONS IN THE ANGLE BETWEEN THE FAILURE PLANE AND BEDDING (γ).

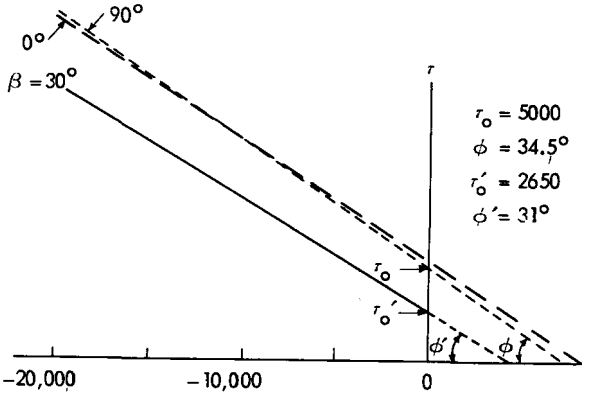

FIG. 18 — MOHR'S ENVELOPES FOR PERMIAN SHALE FOR $\beta = 0°$ AND 30°.

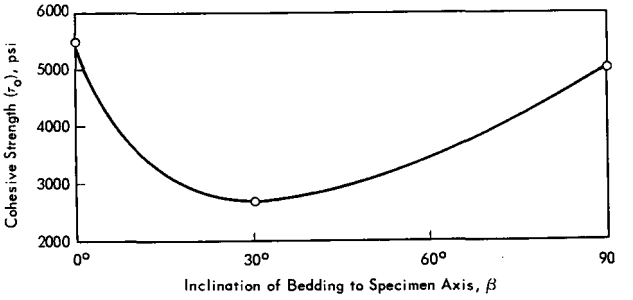

FIG. 19 — VARIATIONS OF SHEAR STRENGTH (τ_o) WITH INCLINATION OF BEDDING (β) FOR PERMIAN SHALE.

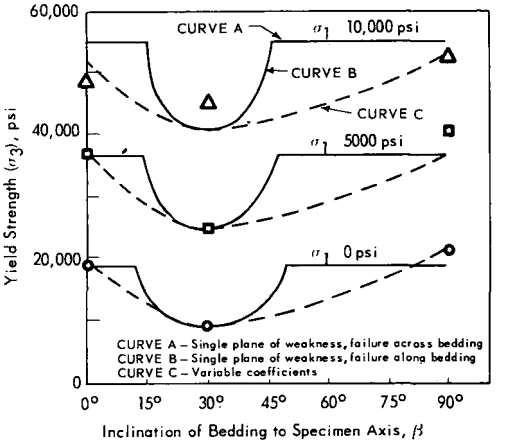

FIG. 20 — COMPARISON OF PERMIAN SHALE EXPERIMENTAL DATA TO SINGLE-PLANE-OF-WEAKNESS THEORY AND VARIABLE-COEFFICIENTS (τ_o AND tan ϕ) THEORY AT VARIOUS CONFINING PRESSURES (σ_1) AND INCLINATIONS OF BEDDING PLANES (β).

with data at $\beta = 0°$, $30°$ and $90°$ gives a maximum and minimum value of yield strength to be expected at a particular orientation for this rock.

In routine analysis of any rock a testing procedure as performed on this shale would be very beneficial in determining whether or not the rock under investigation may be treated as being mechanically isotropic.

TENSILE STRENGTH ANISOTROPIES

A few determinations of tensile strength at atmospheric pressure were made for the laminated rocks using the diametral compression method. This method was originally derived[21] for isotropic media which makes its application to laminae questionable. Justification of its use lies in the assumption that, although the strain distribution in strained anisotropic rocks is not described by a simple Mohr circle, the stress distribution is. The results summarized in Table 2 clearly show that tensile strength also varies appreciably with specimen orientation. Since the rocks used in this study were highly competent, the variations of Table 2 are believed to be conservative.

CONCLUSIONS

On the basis of the rocks tested, the following conclusions have been reached.

1. The simple isotropic elastic model of classical elasticity is probably inadequate for describing the elastic behavior of typical shales, and may be appreciably in error for other rocks showing visible laminations.

2. Bedded rocks can probably be represented by four instead of nine elastic constants as required for an orthotropic body. This is suggested by the isotropic nature of the rocks tested within the X-Z (bedding) plane.

3. Young's modulus is not significantly affected by confining pressure.

TABLE 2 — TENSILE STRENGTHS DETERMINED BY THE DIAMETRAL-COMPRESSION METHOD

	Arkansas Sandstone	Green River Shale	Permian Shale
Failure Plane Perpendicular To Bedding, psi (Arithmetic Mean)	1,698	3,136	2,500
Number of Tests	10	10	3
Standard Deviation, psi	±247	±404	±35
Failure Plane Parallel to Bedding, psi (Arithmetic Mean)	1,387	1,971	1,661
Number of Tests	4	6	3
Standard Deviation, psi	±177	±446	±379
Per Cent Decrease in Tensile Strength with direction	18	37	34

4. Griffith's failure theory may apply quite well to isotropic rocks, as suggested by the behavior of Leuders limestone.

5. The failure behavior of anisotropic laminated rocks may be described by the single-plane-of-weakness theory of Jaeger or by the variable-coefficients approach, depending on the behavior of the rock properties of cohesive strength and coefficient of internal friction with direction.

6. The compressive yield strength of laminated rocks is expected to be higher for specimens cored parallel rather than perpendicular to bedding, as explained from a mechanistic point of view. This strength increase is possibly caused by an increase in the coefficient of friction which arises from the interlocking of individual lamina as the failure surfaces slide along each other.

7. The laminated rocks studied, and possibly most other laminated rocks, are considerably weaker in both compression and tension when failure occurs along the bedding planes.

ACKNOWLEDGMENT

The authors are greatly indebted to many people and organizations who contributed to this study over a three-year period. Portions of the work were supported by API under Project 67E. Additional financial support was furnished at various times by the University Research Institute of The U. of Texas, the Servco Co., the Humble Oil & Refining Co., and the Gulf Oil Foundation. The advice and counsel of the Production Research Div. of The Atlantic Refining Co., the Research Engineering Dept. of Hughes Tool Co., and the Production Research Div. of the Humble Oil & Refining Co. are also acknowledged. Special thanks is also extended to Humble for certain experimental equipment.

NOMENCLATURE

C = elastic shearing constant, psi
E_i = Young's modulus in direction i, psi
K = uniaxial tensile strength, psi
P_c = confining pressure (σ_1), psi
X, Y, Z = orthotropic cartesian coordinates
α = shearing strain, in./in.
β = inclination of anisotropy to cylindrical axis of specimen, degrees
γ = inclination of anisotropy to failure plane, degrees
ϵ_i = strain in direction i, in./in.
θ = angle made by failure plane and minimum principal stress, degrees
ν_{ji} = Poisson's ratio, equal to ϵ_i divided by ϵ_j
σ_n = normal stress, psi
σ_1 = maximum normal stress (P_c), psi
σ_3 = minimum normal stress, psi
τ = shear stress, psi

τ_o = cohesive strength of material, psi

τ_o' = cohesive strength along plane of weakness, psi

ϕ = angle of internal friction in material, degrees

ϕ' = angle of internal friction along plane of weakness, degrees

REFERENCES

1. Handin, J. W. and Hager, R. V., Jr.: "Experimental Deformation of Sedimentary Rocks under Confining Pressure: Test at Room Temperature on Dry Samples", *Bull.* AAPG (1957) Vol. 41, 1.
2. Handin, J. W., Hager, R. V., Jr., Friedman, M. and Feather, J. N.: "Experimental Deformation of Sedimentary Rocks under Confining Pressure: Pore Pressure Tests", *Bull.* AAPG (1963) Vol. 47, No. 5, 717.
3. Robinson, L. H., Jr.: "Effects of Pore and Confining Pressures on Failure Characteristics of Sedimentary Rocks", *Trans.*, AIME (1959) Vol. 216, 26.
4. Griggs, D. T. and Miller, W. B.: "Deformation of Yule Marble: Part I, Compression and Extension Experiments on Dry Yule Marble at 10,000 Atmospheres Confining Pressure, Room Temperature", *Bull.*, G.S.A. (1951) Vol. 62, 853.
5. Bott, M. H. P.: "The Mechanics of Oblique Slip Faulting", *Geol. Mag.* (1959) Vol. 96, 109.
6. Jaeger, J. C.: "Shear Failure of Anisotropic Rocks", *Geol. Mag.* (1960) Vol. 97, 65.
7. Donath, F. A. and Cohen, C. I.: "Anisotropy and Failure in Rocks", (Abstract) *Bull.*, GSA (1960) Vol. 71, 1851.
8. Donath, F. A.: "Experimental Study of Shear Failure in Anisotropic Rocks", *Bull.*, GSA (1961) Vol. 72, 985.
9. Adler, L.: "Failure in Geologic Materials Containing Planes of Weakness", *Trans.*, AIME (1963) Vol. 226, 88.
10. Kalinin, A. G. and Belorussov, V. O.: "Effect of Rock Anisotropy on the Deviation of Wells", *Neft. Khoz.* (March, 1963) No. 3, 8.
11. Sokolnikoff, I. S.: *Mathematical Theory of Elasticity*, Second Ed., McGraw-Hill Book Co. Inc., N.Y. (1956).
12. "Stress-Strain Relations in Wood and Plywood Considered as Orthotropic Materials", Forest Products Laboratory, U. S. Dept. of Agriculture Forest Service, Report No. 1503 (March, 1956; orig. publ. 1944).
13. Chenevert, M. E.: "The Deformation-Failure Characteristics of Laminated Sedimentary Rocks", PhD Dissertation, The U. of Texas (Jan., 1964).
14. Griffith, A. A.: "The Theory of Rupture", *Proc.*, First Int. Cong. for Applied Mech., Delft (1924) 55.
15. Gray, K. E.: "Fixed-Blade Planing of Rocks in the Brittle Stress State", PhD Dissertation, The U. of Texas (1963).
16. Garner, N. E.: "Experimental Study of Crater Formation in Rocks at Elevated Stress States", PhD Dissertation, The U. of Texas (1963).
17. Crisp, H. A.: "Additional Studies: Fixed Blade Planing of Rocks in the Brittle Stress State", MS Thesis, The U. of Texas (1963).
18. Hetenyi, M.: *Handbook of Experimental Stress Analysis*, John Wiley & Sons Inc., N. Y. (1950) 7.
19. Robertson, E. C.: "Experimental Study of the Strength of Rocks", *Bull.*, G.S.A. (1955) Vol. 66, 1275.
20. Bowen, F. P. and Tabor, D.: *The Friction and Lubrication of Solids*, Oxford Press, London (1950) 169-175.
21. Den Hartog, J. P.: *Advanced Strength of Materials*, First Ed., McGraw-Hill Book Co., Inc., N. Y. (1952) 200.

APPENDIX

ELASTIC CONSTANTS MEASUREMENTS

All formations tested displayed compositional variations, as well as anisotropic effects. Table A-1 lists the arithmetic mean, number of tests and standard deviation for each direction tested. ***

TABLE A-1

Elastic Parameters	Arithmetic Mean	No. of Tests	Std. Div.	Arithmetic Mean	No. of Tests	Std. Div.
	Leuders Limestone			Arkansas Sandstone		
E_y	3.52×10^6, psi	20	±0.462	2.82×10^6, psi	3	±0.027
E_x	3.71	16	.375	4.53	3	.072
E_z	3.59	14	.505	4.76	3	.146
ν_{yx}	.20	4	.027	.14	3	.011
ν_{yz}	.20	4	.027	.11	3	.004
ν_{xy}	.185	4	.019	.21	3	.006
ν_{zy}	.23	3	.020	.18	3	.015
ν_{zx}	.23	3	.020	.15	3	.002
ν_{xz}	.19	4	.010	.14	3	.009
	Green River Shale			Permian Shale		
E_y	4.27×10^6, psi	13	±0.389	3.54×10^6, psi	3	±0.087
E_x	5.11	11	.476	5.13	3	.104
E_z	5.08	12	.606	4.58	3	.125
ν_{yx}	.18	4	.009	.13	3	.007
ν_{yz}	.18	2	.010	.13	3	.010
ν_{xy}	.18	6	.016	.21	3	.017
ν_{zy}	.19	4	.014	.21	3	.016
ν_{zx}	.16	5	.009	.18	3	.007
ν_{xz}	.15	6	.010	.17	3	.012